European Journal of Medicinal Chemistry 93 (2015) 83–92

Contents lists available at ScienceDirect

European Journal of Medicinal Chemistry

journal homepage: http://www.elsevier.com/locate/ejmech

Original article

Synthesis and biological evaluation of pyridazino[1′,6′:1,2]pyrido[3,4-*b*]indolinium and pyridazino[1,6-*a*]benzimidazolium salts as anti-inflammatory agents

Aranzazu Rodríguez-Sanz [a], Patricia Sánchez-Alonso [b], Teresa Bellón [a, **], Ramón Alajarín [b, *], Virginia Martínez-Cabeza [a], Rafael Selgas [c], Juan J. Vaquero [b], Julio Álvarez-Builla [b]

[a] Instituto de Salud Hospital Universitario La Paz – IdiPAZ, Madrid, Spain
[b] Departamento de Química Orgánica y Química Inorgánica, Universidad de Alcalá, Madrid, Spain
[c] Hospital Universitario La Paz, Servicio de Nefrología, IdiPAZ, IRSIN, Madrid, Spain

ARTICLE INFO

Article history:
Received 20 October 2014
Received in revised form
27 January 2015
Accepted 30 January 2015
Available online 31 January 2015

Keywords:
Anti-inflammatory
TNF-α
Cytokine
Pyridazino[1′,6′:1,2]pyrido[3,4-*b*]indolinium
Pyridazino[1,6-*a*]benzimidazolium

ABSTRACT

Condensed polycyclic heteroaromatic cations bearing a bridgehead nitrogen with pyridazino[1′,6′:1,2]pyrido[3,4-*b*]indolinium and pyridazino[1,6-*a*]benzimidazolium structures were assayed as inhibitors of LPS-induced TNF-α production by THP-1 cells. The hit compound **1e**, which had the best IC_{50} value (4.49 μM) and low toxicity, was further assayed on human PMBCs (IC_{50} 3.91 μM) and monocytes (IC_{50} 1.82 μM). This compound also inhibited TNF-α production following poly I:C stimulation of human monocytes and monocyte-derived dendritic cells; in the latter case, inhibition of IL-12 production was also observed. Compound **1e** was also able to inhibit TNF-α expression at the transcriptional level and proved to be effective *in vivo*. Compound **1e** is an interesting potential therapeutic agent in IMIDs.

1. Introduction

Inflammation is a complex and dynamic physiological process that occurs in response to cell or tissue damage and is an attempt to defend the body against external aggression. However, chronic inflammation may be pathological. Immune-mediated inflammatory disorders (IMIDs) are lifelong conditions that cause substantial morbidity and disability [1]. Tumour necrosis factor alpha (TNF-α) is a potent multifunctional cytokine that plays a pivotal role in the inflammatory response and it is mainly secreted by macrophages upon stimulation by danger signals or bacterial products such as lipopolysaccharides (LPS) [2]. TNF-α is involved in the regulation of a broad spectrum of biological processes such as cell proliferation, differentiation, apoptosis, and lipid metabolism [3]. TNF-α stimulates angiogenesis and, in combination with other proinflammatory cytokines, can provoke alterations in endothelial cells leading to several pathologies involving the microvasculature. Given its involvement as a master regulator of other inflammatory cytokines, TNF-α has been postulated to be the most important cytokine in the pathogenesis of IMIDs [4], including autoimmune diseases, insulin resistance, and cancer [5].

There is evidence to suggest that chronic inflammation has a pathological role in obesity and type 2 diabetes (T2D). Interactions between the inflammatory response and metabolism take place preferentially in adipose tissue, which is composed of adipocytes and immune cells such as macrophages [6]. TNF-α protein is also highly expressed in the adipose tissue of obese animals or humans

Abbreviations: AP, activation protein; BBDECl, 1,5-bis-[*N*-benzyl-*N*,*N*-diethylammonium)-3-oxapentane dichloride; CBA, cytometric bead array; DC, dendritic cell; IMIDs, immune mediated inflammatory diseases; JNK, c-Jun N-terminal kinase; LPS, lipopolysaccharide; MSH, *O*-(mesitylsulfonyl)hydroxylamine; μW, microwaves; NF-κB, nuclear factor κB; PBMCs, peripheral blood mononuclear cells; RT-PCR, real-time polymerase chain reaction; SD, supplementary data; TACE, TNF-α converting enzyme; TNF, tumour necrosis factor; TNFR, tumour necrosis factor receptor; T2D, type 2 diabetes.

* Corresponding author. Departamento de Química Orgánica y Química Inorgánica, Universidad de Alcalá, 28871 Alcalá de Henares, Madrid, Spain.
** Corresponding author. Institute for Health Research, Hospital Universitario La Paz – IdiPAZ, Paseo Castellana 261, Madrid, Spain.
E-mail addresses: teresa.bellon@salud.madrid.org (T. Bellón), ramon.alajarin@uah.es (R. Alajarín).

http://dx.doi.org/10.1016/j.ejmech.2015.01.060
0223-5234/

with T2D and it contributes significantly to insulin resistance, because the administration of recombinant TNF-α results in a resistance to insulin action [7]. Furthermore, a blockade of the biochemical, genetic, or pharmacological actions of TNF-α results in greatly increased insulin sensitivity [8]. Therefore, inhibition of the over-expression of TNF-α might be an effective strategy for the prevention and treatment of metabolic and immune-mediated diseases.

Inhibition of TNF-α activity by humanised monoclonal antibodies or soluble receptors has been effective in treating IMIDs, thus supporting the pivotal role of TNF-α in the pathogenesis of these diseases [4,9]. Despite the success achieved with biological drugs, their requirement of delivery by injection and the associated high costs have limited their use. Moreover, these biotechnological drugs are immunogenic, and some patients who receive long-term treatment will develop anti-drug antibodies, which in turn will lead to a loss of response [10]. Although synthetic antibodies such as etanercept, infliximab, and adalimumab have been approved for the treatment of inflammatory diseases by direct inhibition of TNF-α, small-molecule inhibition to block either the function or the production of TNF-α may prove to be an alternative solution. This challenging field is still in its infancy and efforts have typically been limited to inhibitors of the processing TNF-α converting enzyme (TACE), i.e., uncharacterised inhibitors of TNF-α expression or cell-based assays, and intracellular pathway inhibitors that antagonise nuclear factor κB (NF- κB), activation protein 1 (AP 1), or c-Jun N-terminal kinase (JNK)/p38 signal transduction [11]. To date, very few molecule-based inhibitors have been reported for the inhibition of *in vitro* TNF receptor 1 (TNFR1) binding to TNF-α, which is an interesting new approach that involves protein–protein binding inhibition [12,13]. Some inhibitors bearing quinazolinone [14,15], quinuclidine, or quinolizine [16] frameworks proved to bind TNF-α *in silico*. The strongest small-molecule TNF-α inhibitor reported to date, SPD304, promotes subunit disassembly of this trimeric

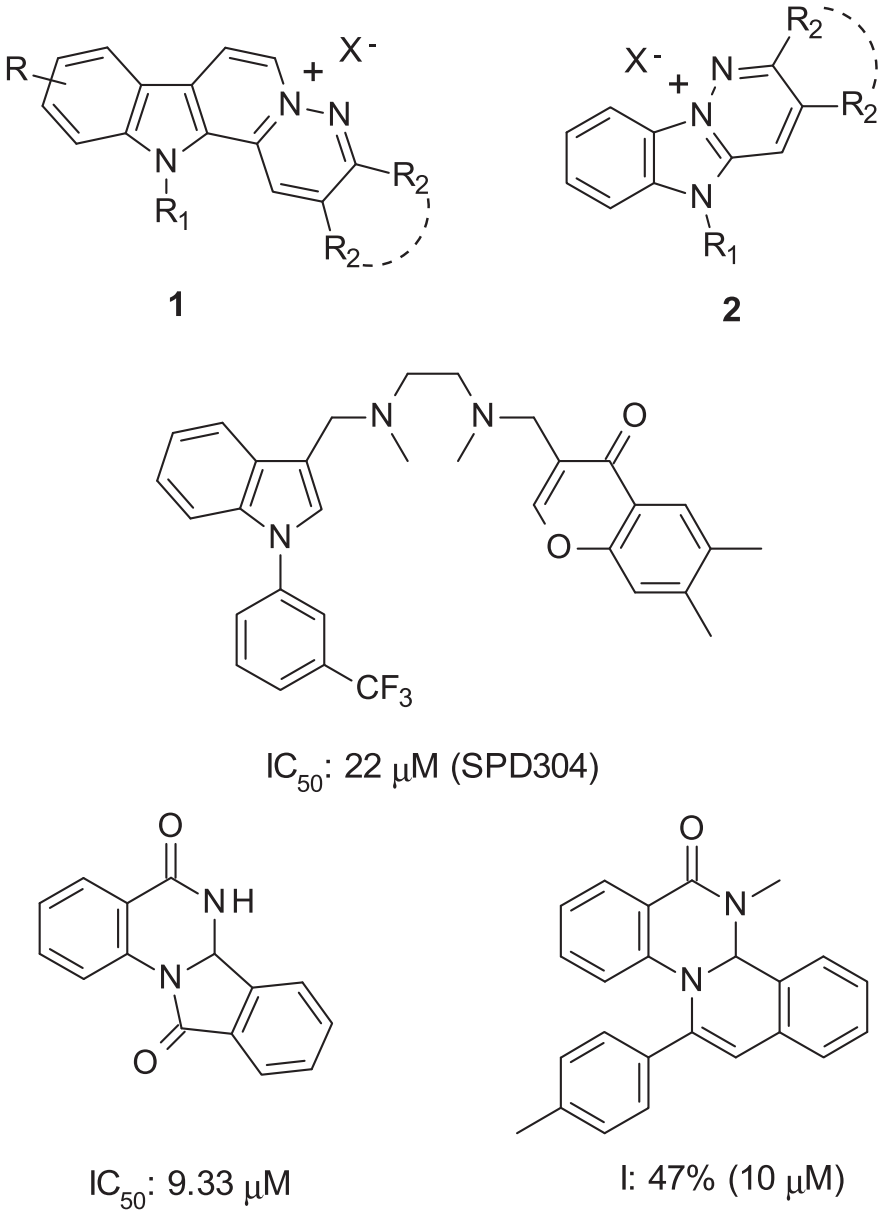

Fig. 1. General chemical structures of **1** and **2** and some TNF-α inhibitors. Indole-coumarin (SPD304), an inhibitor of TNFR1 binding to TNF-α, isoindolo[2,1-*a*]quinazolinedione (bottom left) and isoquinolino[2,1-*a*]quinazolinone (bottom right), inhibitors of TNF-α production.

cytokine [17] (Fig. 1).

Herein we report on a study on the anti-inflammatory potency of a series of new and known pyridazino[1′,6′:1,2]pyrido[3,4-*b*]indolinium salts **1** and pyridazino[1,6-*a*]benzimidazolium salts **2** (Fig. 1). The anti-inflammatory effect was measured by the inhibition of LPS-induced TNF-α production. Furthermore, the *in vivo* anti-inflammatory effect of a selected inhibitor was also analysed.

2. Chemistry

The designed structures were divided into two classes: pyridazino[1′,6′:1,2]pyrido[3,4-*b*]indolinium salts **1** and pyridazino[1,6-*a*]benzimidazolium salts **2**. We previously described the synthesis of these types of compounds. Some of the examples proved to be DNA-intercalators and cytotoxic agents against leukaemia L1210 and colon carcinoma HT-29 cell lines [18,19]. We previously described compounds **1a**–**d** and **1f**,**g**, and they were re-synthesised in this study (Scheme 1) [18]. Experimental procedures and spectroscopic and analysis data for these compounds and their intermediates are provided in the supplementary data (SD) appendix. The starting materials were the commercially available β-carboline-type natural products harmane (**3**), harmol (**4**), and harmine (**5**). The reaction sequence was a combination of *N*-alkylation or *N*-acylation at the azole nitrogen, *N*-amination at the azine nitrogen and Westphal condensation with a 1,2-diketone. The carbocyclic ring of harmane (**3**) was functionalised by electrophilic aromatic substitution and the hydroxyl group of harmol (**4**) was alkylated by Williamson reaction.

A similar synthetic strategy was applied to the preparation of other compounds in this series (Scheme 2). Compound **1h** was prepared by alkylation with 1,3-diiodopropane from **8**, which was synthesised as reported earlier (see SD) [18]. Compound **1i** was prepared by acidic hydrolysis of **1f**. Compound **9** was obtained by alkylation of harmine (**5**) using phase-transfer catalysis (PTC) conditions [20] followed by treatment with *O*-(mesitylsulfonyl) hydroxylamine (MSH) to give **10** (see SD). Subsequent basic condensation with acenaphthoquinone gave **1j**. Treatment of compound **9** with copper(II) acetate gave the dimeric compound **11**. Subsequent amination to give **12** followed by basic condensation with hexane-3,4-dione yielded **1k**.

The series of pyridazino[1,6-*a*]benzimidazolium salts **2** was prepared from 2-methyl-benzimidazole (**13**) in a reaction sequence that involved *N*-alkylation, *N*-amination, and basic condensation with acenaphthoquinone. Compounds **14** and **15** were prepared as reported previously [19,21]. Acidic hydrolysis provided **2a** and **2b**, respectively. The reaction of **2a** with thionyl chloride gave **16** [22], which was alkylated with 1,3-dibromopropane to give **17**. Subsequent treatment with *N*,*N*,*N*,*N*-tetramethyl-propane-1,3-diamine gave **2c** (Scheme 3).

3. Results and discussion

3.1. Determination of THP-1 cell line viability in the presence of compounds *1* and *2*

Monocytes and macrophages are the main producers of TNF-α. The human monocytic cell line THP-1 was used to explore the potential activity of compounds **1** and **2** as TNF-α synthesis inhibitors. Previous data showed the putative cytotoxic potential of indolinium and benzimidazolium derivatives [18,19]. The potential

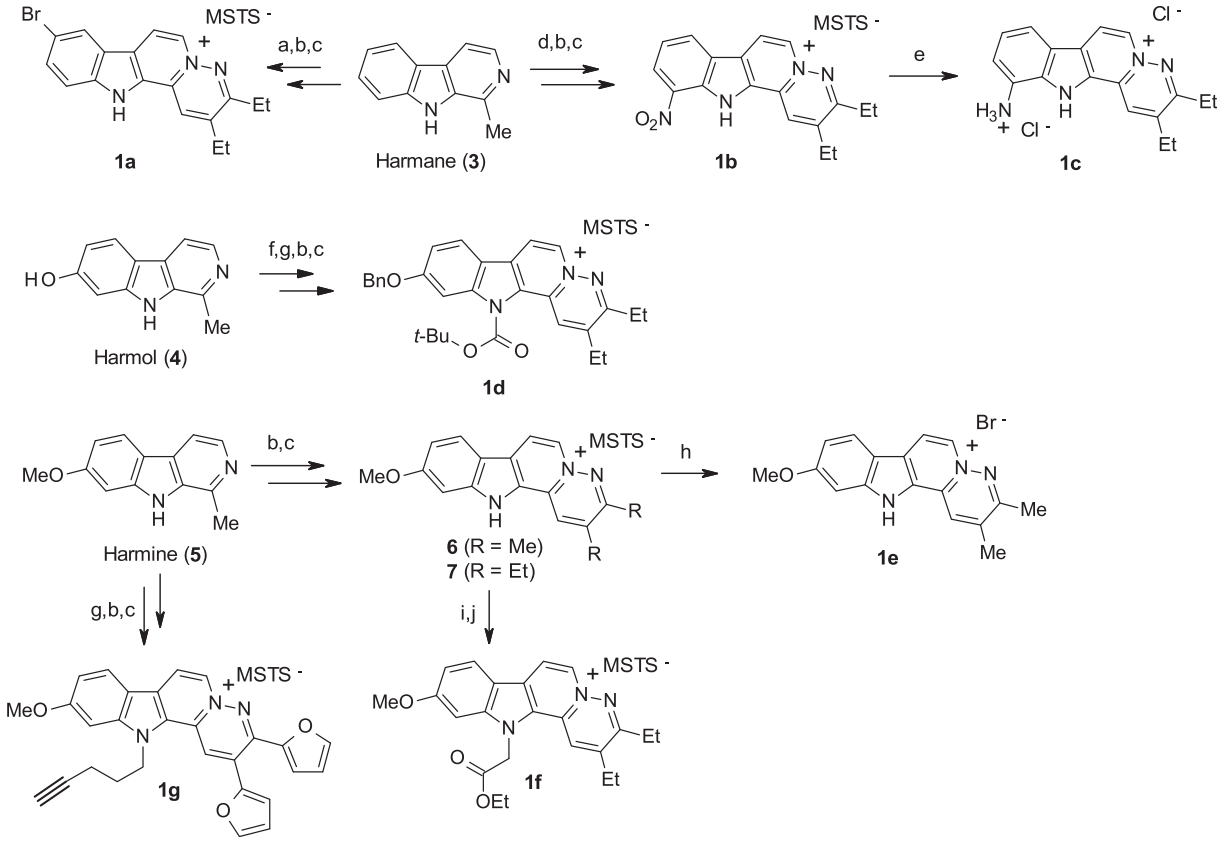

Scheme 1. Synthetic pathway for compounds **1a**–**g**. *Reagents and conditions* (see SD and ref. 18): a) Br_2, THF; b) MSH, CH_2Cl_2; c) 1,2-diketone, Et_3N or AcONa, EtOH or acetone, reflux; d) HNO_3, 0 °C; e) $SnCl_2$, HCl, reflux; f) Boc_2O, Et_3N, DMAP, CH_2Cl_2; g) RBr, KOH, K_2CO_3, BBDECl, MeCN; h) 48% HBr; i) Et_3N, H_2O; j) Ethyl bromoacetate, MeCN.

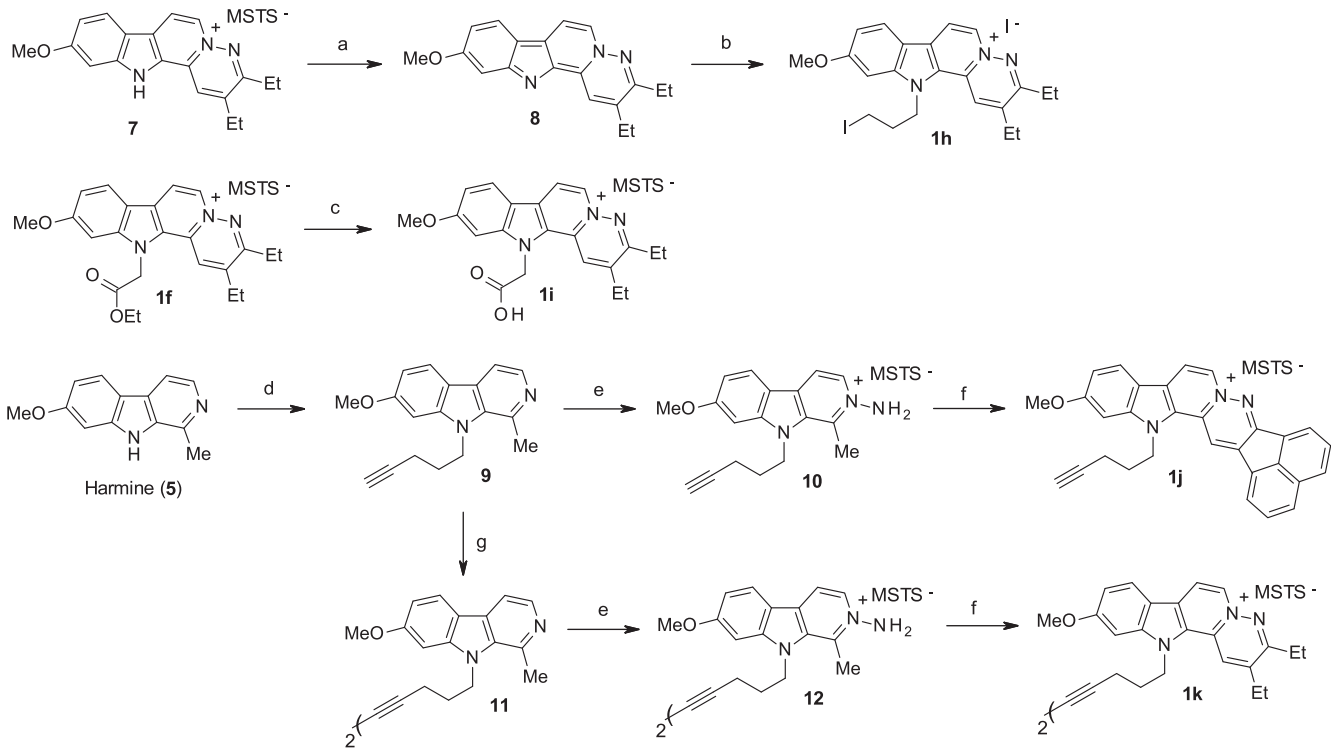

Scheme 2. Synthetic pathway for compounds **1h**–**k**. *Reagents and conditions*: a) Et_3N, H_2O; b) 1,3-diiodopropane, 300 W, μW, two runs; c) 48% HBr, reflux; d) 5-chloro-pent-1-yne, BBDECl, NaOH, K_2CO_3, MeCN; e) MSH, CH_2Cl_2; f) 1,2-diketone, CH_3CO_2Na, EtOH, reflux; g) $Cu(AcO)_2$, CH_3CN, reflux.

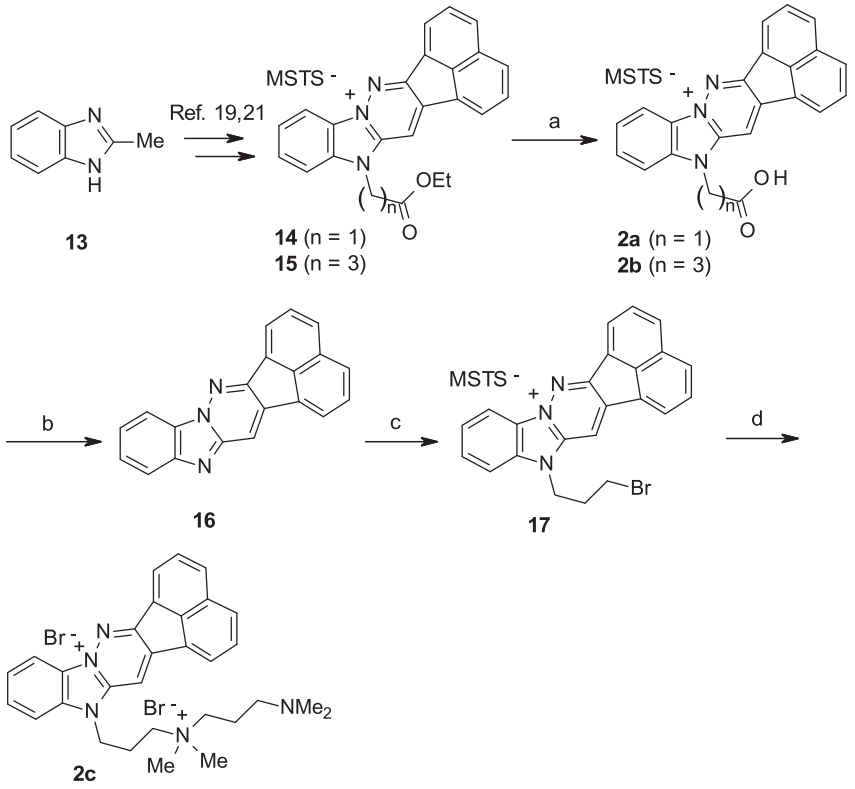

Scheme 3. Synthetic pathway for compounds **2a**–**c**. *Reagents and conditions*: a) 48% HBr, reflux; b) **2a**, $SOCl_2$, reflux; c) 1,3-dibromopropane, 300 W, μW; d) *N*,*N*,*N*,*N*-tetramethylpropane-1,3-diamine, DMF, 100 °C.

cytotoxicity of these newly synthesised molecules was analysed by incubating THP-1 cells for 24 h in the presence of each compound (10 μM) and the cell viability was then assessed. Parallel cultures were established, in which cells were further stimulated with 100 ng/mL of LPS during the last 4 h to rule out the deleterious effect of an inflammatory challenge. Differences were not observed between cultures with and without LPS (data not shown). The cell viability of LPS-stimulated cells preincubated for 24 h with compounds **1** or **2** (10 μM) is represented in Fig. 2.

3.2. In vitro inhibition assay of LPS-induced TNF-α production

The ability of the various compounds to modulate the production of TNF-α was first explored in THP-1 cells. Cells were pretreated or left untreated overnight in the presence of increasing concentrations of each compound and were then further stimulated with LPS for 4 h. Preliminary experiments were performed in which one single dose of 10 μM was analysed. Further experiments with increasing concentrations were performed only with those compounds that showed low toxicity (**1b**, **1c**, **1e**, **1f**, **1h**, **1i**, **2a**, **2b**). The results are summarised in Table 1.

3.3. Structure–activity relationships

Although the number of compounds synthesised and tested was small, several tentative relationships can be established for the cell viability and TNF-α production inhibition data. For series **1** (see Fig. 2 and Table 2), the presence of a 9-Br substituent in R made cells unviable (**1a**), although this was possibly a consequence of the labile nature of the bromo-substituent rather than the position itself. The presence of nitro, ammonium or short-chain alkoxy groups at positions C-10 or C-11 was relatively well tolerated (**1b**, **1c**, **1e**). In the R_1 substituent, the presence of an alkyne moiety was detrimental as compounds **1g**, **1j**, **1k** are highly toxic. Indeed, alkynes are well-known DNA-photocleaving agents [23] and terminal alkynes have recently been reported to be acceptors of the active-site cysteine nucleophile [24]. The presence of hydrogen and non-bulky short-chain ester or carboxylic acid groups was well tolerated (**1b**, **1c**, **1e**, **1f**, **1i** *vs.* **1d**) although a haloalkyl chain reduced viability (**1f**, **1i** *vs.* **1h**). A similar effect was also observed in series **2** (**2a**, **2b** *vs.* **2c**) and this was probably a consequence of the alkylating potential of **1h** and **2c**.

For compounds that showed cell viability above 50% (**1b**, **1c**, **1e**, **1f**, **1h**, **1i**, **2a**, **2b**; Tables 1 and 2), increasing concentrations were tested in order to calculate the IC_{50} values. Compounds **1b**, **1c**, and **1i** did not show dose-dependent inhibition. Within series **1**, the presence of a hydrogen substituent at R_1 (**1e**, IC_{50} = 4.49 μM) provided better inhibition than an ethoxycarbonylmethyl chain (**1f**, IC_{50} = 11.5 μM) or a 3-iodopropyl chain (**1h**, IC_{50} = 9.88 μM). Within series **2**, the presence of a shorter carboxyalkyl chain was preferred (**2a**, IC_{50} = 14.6 μM; **2b**, IC_{50} = 39.2 μM).

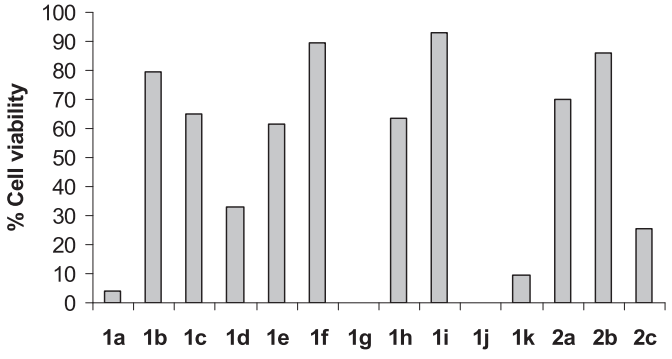

Fig. 2. Cell viability of LPS-stimulated cells preincubated with compounds **1** or **2** (10 μM). THP-1 cells were incubated overnight in the presence of the indicated compounds followed by 4 h of stimulation with 100 ng/mL LPS. Cell line viability was evaluated by exclusion of propidium iodide as measured by flow cytometry.

Table 1
Inhibitory activity (% inhibition of TNF-α production) and toxicity (% cell viability) of compounds **1** and **2** in THP-1 cells.

N[a]	Compd.	Inhibition (%) *vs.* concentration (μM)[b]							IC_{50} (μM)	Cell viability (%)[c]
		0.1	1	5	10	25	50	100		
1	**1a**				89					3.76
2	**1b**		44	56	29	47				79.36
1	**1c**		13.3	−13.4	88					65.02
1	**1d**				94					33.05
9	**1e**	−0.97	34.9	63.4	87.8				4.49	61.27
3	**1f**		51	67	45	94			11.5	89.72
1	**1g**				87					0
2	**1h**		11	36	72	79			9.88	63.28
5	**1i**				38	29	35	40		93
1	**1j**				94					0
1	**1k**				34					9.54
3	**2a**	9	12	7	45	84			14.6	69.91
6	**2b**				19	47	70	85	39.2	86
2	**2c**				39					25.28

[a] No. of experiments performed with each compound.
[b] Inhibition of TNF-α production in response to 100 ng/mL LPS. Mean values corresponding to a number of independent experiments indicated in the left-hand column are shown.
[c] % cell viability of cells incubated with 10 μM of compounds plus 100 ng/mL LPS.

3.4. Inhibitory effect of *1e* in LPS-induced TNF-α production by THP-1 and primary human cells

Of the compounds analysed, **1e** showed the lowest IC_{50} value in the monocytic cell line THP-1. As a consequence, we decided to test the ability of **1e** to downregulate TNF-α production by primary human peripheral blood mononuclear cells (PBMCs) and purified human monocytes. As can be seen from Fig. 3, a dose-dependent inhibition of TNF-α production was observed in PBMCs and in human $CD14^+$ monocytes as well as in THP-1 cells. The IC_{50} values were calculated in PBMCs and human monocytes (Table 3).

3.5. Inhibitory effect of compound *1e* on poly I:C-induced TNF-α and IL-12 production by human monocytes and in vitro differentiated myeloid dendritic cells (DCs)

Poly I:C is a synthetically produced mimetic of viral RNA that is also able to stimulate the inflammatory response in monocytes,

Table 2
Substituents at positions R, R_1, and R_2 for compounds **1** and **2**.

Compd.	R	R_1	R_2
1a	9-Br	H	Et
1b	11-NO_2	H	Et
1c	11-$(NH_3)^+$	H	Et
1d	10-BnO	CO_2Bu^t	Et
1e	10-MeO	H	Me
1f	10-MeO	CH_2CO_2Et	Et
1g	10-MeO	$HCC(CH_2)_3$	2-Furyl
1h	10-MeO	$I(CH_2)_3$	Et
1i	10-MeO	CH_2CO_2H	Et
1j	10-MeO	$HCC(CH_2)_3$	1,8-Dinaphthyl
1k	10-MeO	$(CH_2)_3CC(CH_2)_3$	Et
2a	–	CH_2CO_2H	1,8-Dinaphthyl
2b	–	$(CH_2)_2CO_2H$	1,8-Dinaphthyl
2c	–	$Me_2N(CH_2)_3N^+Me_2(CH_2)_3$	1,8-Dinaphthyl

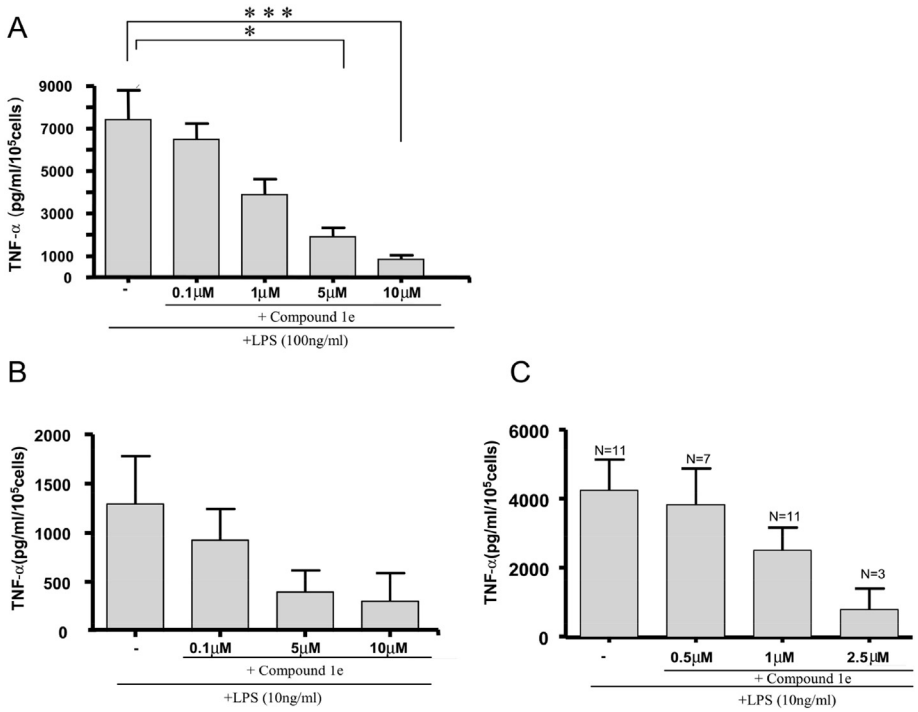

Fig. 3. Dose-dependent inhibition of TNF-α production by **1e**. (A) THP-1 cells; (B) human peripheral blood mononuclear cells (PBMCs); (C) $CD14^+$ human monocytes. Cells were cultured overnight with increasing concentrations of **1e**, followed by LPS stimulation for 4 h. TNF-α production was quantified by ELISA in the culture supernatants. *P value < 0.05 and ***P < 0.001 (Kruskal–Wallis and Dunns post-test).

Table 3
Inhibition of TNF-α production by **1e** in human primary cells.

	1e (μM)						IC_{50} (μM)
	0.1	0.5	1	2.5	5	10	
% I (PMBCs)[a]	22.7	nd	38.8	nd	71.2	69.2	3.91
% I (monocytes)[a]	nd	28.56	38.15	56.41	nd	95.3	1.82

[a] Inhibition of TNF-α production in response to 100 ng/mL LPS; nd. Not determined.

macrophages, and dendritic cells. The functional capability of **1e** to dampen inflammation triggered by various stimuli was assessed by pretreating human monocytes and monocyte-derived dendritic cells with **1e** and then challenging them with poly I:C. Fig. 4 shows that **1e** was able to inhibit the production of TNF-α triggered by poly I:C in monocytes and dendritic cells. Furthermore, pretreatment with low doses of **1e** was also able to inhibit the production of IL-12 in poly I:C stimulated DCs.

3.6. Inhibition of TNF-α transcription by *1e* in human monocytes

Transcriptional and post-transcriptional mechanisms are involved in regulating the production of TNF-α by immunocytes. Real-time RT-PCR studies were performed to explore whether **1e** was able to inhibit the expression of TNF-α at the transcriptional level. Fig. 5 shows that LPS induction of TNF-α mRNA was almost completely abrogated in monocytes pretreated with 1 μM of **1e**.

3.7. In vivo anti-inflammatory activity of *1e*

Previous data demonstrate the inhibitory effect of **1e** *in vitro*. The efficacy of the compound administered *in vivo* was investigated by administering two doses of **1e** (2 mg/kg) intraperitoneally to C57BL/6 mice at an interval of 18 h. The animals were sacrificed 4 h after the second dose. The spleen cells were then isolated and cultured *in vitro* in the presence or absence of LPS. The production of TNF-α was measured in the culture supernatants by flow cytometry CBA. LPS significantly stimulated the production of TNF-α in cells from vehicle-treated mice, but it was no longer able to stimulate a significant increase in TNF-α production by splenocytes when mice had been injected with **1e**. As a result, the release of TNF-α in response to LPS was significantly reduced in cells from treated mice compared to the control group (Fig. 6). These data strongly suggest that *in vivo* administration of **1e** was able to reduce the response of immune cells to a strong proinflammatory stimulus such as LPS.

4. Conclusions

In summary, 14 compounds were prepared and their toxicity and ability to dampen the inflammatory response was evaluated by measuring the inhibition of the production of the pleiotropic cytokine TNF-α. Several derivatives showed inhibitory activity, but **1e** was selected for further study based on its low toxicity and efficacy at a low concentration (IC_{50} = 4.49 μM) in THP-1 cells. Moreover, compound **1e** was even more potent in isolated human monocytes (IC_{50} = 1.82 μM) and proved to be effective *in vivo*. In addition to inhibiting inflammatory signals delivered by a bacterial component such as LPS, compound **1e** also downregulated the production of proinflammatory cytokines in response to a viral-mimicking stimulus such as poly I:C, which is an analogue of viral ssRNA. Furthermore, this compound not only downregulated TNF-α production by macrophages, but was also able to inhibit the production of a founder proinflammatory cytokine such as IL-12 by stimulated dendritic cells. The experimental data suggest that **1e** could be a potential therapeutic agent in IMIDs, for which anti-TNF drugs have been successfully used, as well as for other diseases such as immune reconstitution syndrome, in which additional cytokines

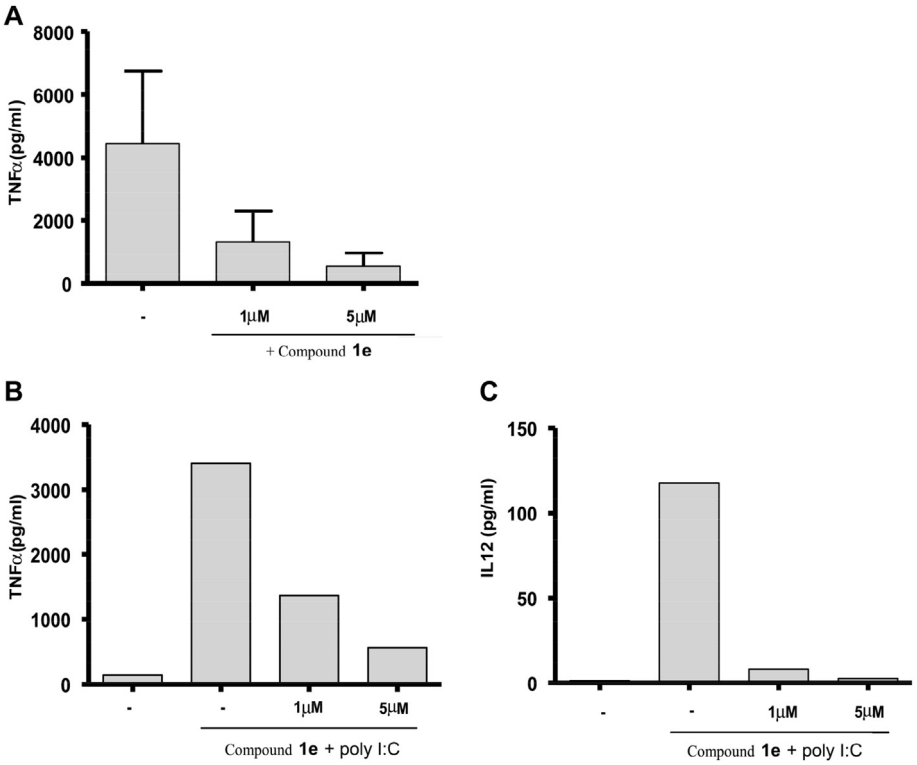

Fig. 4. Inhibition of TNF-α production by **1e**. (A) Purified human monocytes; (B,C) monocyte-derived dendritic cells. Cells were pretreated for 1 h with **1e** at various concentrations followed by overnight poly I:C stimulation. TNF-α and IL-12 production were quantified by ELISA and CBA, respectively, in the culture supernatants. Mean ± SEM values of three independent experiments are shown in A.

may exacerbate the patients' response, or conditions in which inflammatory macrophages may play a role, such as metabolic syndromes.

5. Experimental section

5.1. Chemistry

Solvents (HPLC quality, Scharlab) were dried in a Solvent Purification System (MBraun) by passage through a pre-activated alumina column or they were purchased as anhydrous quality. Reagents were purchased from Sigma–Aldrich and were used as received. The reactions involving moisture-sensitive compounds

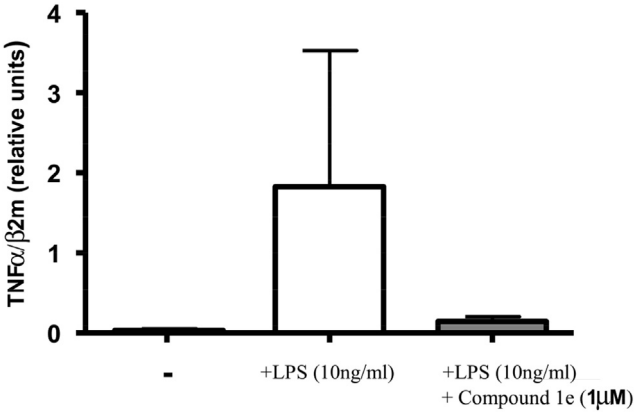

Fig. 5. Inhibition of TNF-α transcription by **1e** in human monocytes. The expression of TNF-α in response to LPS stimulation 10 ng/mL (2 h) was measured by real-time RT-PCR in purified $CD14^+$ human monocytes pretreated overnight with **1e** (1 μM) or left untreated. TNF-α mRNA molecules were normalised to β_2-microglobulin mRNA, which was used as a reference gene. Mean ± SEM values corresponding to 3 independent experiments are shown.

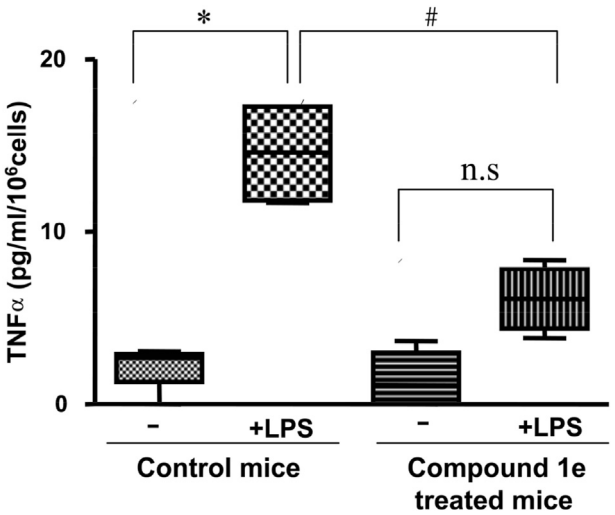

Fig. 6. Analysis of the efficacy of **1e** *in vivo*. Splenocytes from mice treated intraperitoneally with two doses (2 mg/kg) of **1e** or vehicle were isolated and cultured *in vitro* in the presence or absence of 10 ng/mL LPS for 4 h and the secretion of TNF-α was evaluated by CBA. Box plots represent values in culture supernatants from 4 mice in each group. The horizontal middle lines represent the median, the top and bottom lines represent the quartile values, and the T-bars represent the maximum and minimum values. The Wilcoxon matched pair test was used to analyse data obtained within the same group (*p = 0.0156 control *vs.* LPS; n.s.: not significant). The Mann–Whitney U test was applied to compare data from **1e** and vehicle-treated mice (#p = 0.0205 vehicle + LPS *vs.* Compound **1e** + LPS).

were performed under an atmosphere of dry argon. Microwave-assisted reactions were carried out in a 5 mL vial using a Synthewave 402 microwave synthesizer (Prolabo). The reactions were monitored by thin-layer chromatography (TLC) on silica-coated aluminium sheets ($60F_{254}$ Alugram) and chromatograms were visualised with UV light (254 or 366 nm). Purification by column chromatography was undertaken with Merck silica gel (0.030–0.075 mm) and the solvents were used as received (Scharlab). Infrared spectra (IR, KBr window) were recorded on a Perkin–Elmer FTIR 1725X instrument. The frequencies (ν) of the most intense bands are given in cm^{-1}. Nuclear magnetic resonance spectra (^1H and ^{13}C NMR) were recorded using Varian Mercury-VX-300 MHz (300 and 75 MHZ, respectively) and Varian-UNITY^{PLUS}-500 (500 and 125 MHz, respectively) instruments. Chemical shifts (δ) are given in ppm and are referenced to the residual signal of the non-deuterated solvent. Coupling constants (J) are given in Hz. The abbreviations s = singlet, d = doublet, dd = doublet of doublets, t = triplet, td = triplet of doublets, q = quadruplet, m = multiplet, bs = broad signal, appt = apparent triplet are used throughout. Elemental analyses (C, H, N) were carried out on a Heraeus CHN Rapid Elemental Analyzer and were within ±0.4% of the theoretical values.

The supplementary data contains experimental procedures and characterisation data for compounds **1a**–**d**, **1f**–**g**, **16** and their intermediates. ^1H and ^{13}C NMR spectra for **1e** and its intermediates are also provided as representative examples. The synthesis of new compounds **1e**, **1h**–**k** and **2a**–**c** is described below.

5.1.1. 2,3-Dimethyl-12H-10-methoxy-pyridazino[1′,6′:1,2]pyrido[3,4-b]indol-5-inium bromide (*1e*)

A solution of **6** (see SD) (51 mg, 0.1063 mmol) in 48% HBr (2 mL) was stirred at room temperature for 1 h. The solvent was removed under reduced pressure and the residue was dried under a vacuum. The solid was treated with Et_2O in an ultrasound bath and the mixture was filtered. Compound **1e** was obtained as a yellow solid and this was recrystallized from ethanol/acetic acid. Yield: 31%; mp: >280 °C (dec.); ^1H NMR (300 MHz, CD_3OD): δ 9.09 (d, 1H, J = 7.0 Hz), 8.78 (s, 1H), 8.67 (d, 1H, J = 7.0 Hz), 8.32 (d, 1H, J = 9.0 Hz), 7.29 (d, 1H, J = 2.2 Hz), 7.17 (dd, 1H, J = 9.0 Hz, J = 2.2 Hz), 4.03 (s, 3H), 2.84 (s, 3H), 2.73 (s, 3H). ^{13}C NMR (125 MHz, CD_3OD): δ 164.4, 162.1, 146.4, 139.6, 131.7, 131.2, 130.2, 128.6, 127.8, 127.3, 124.4, 117.0, 115.7, 114.8, 100.9, 95.5, 56.4, 20.7, 19.4. HRMS [ESI-TOF]: Calcd for $C_{17}H_{16}N_3O$, [M^+]: 278.1286. Found [M^+]: 278.1288. Anal. ($C_{17}H_{16}BrN_3O$) theoretical: C, 57.00; H, 4.50; N, 11.73. Found: C, 57.27; H, 4.82; N, 11.38.

5.1.2. 2,3-Diethyl-10-methoxy-12-(3-iodopropyl)-pyridazino[1′,6′:1,2]pyrido[3,4-b]indol-5-inium iodide (*1h*)

A slurry of **8** (see SD) (86.8 mg, 0.3 mmol) in 1,3-diiodopropane (5 mL) was irradiated in a microwave synthesiser for 10 min (×2) at 300 W. The solid was filtered when the mixture was still hot and was washed with acetone (2 × 5 mL) and Et_2O (2 × 5 mL). Crystallization from ethanol yielded **1h** as an orange solid. Yield: 55%; mp: >300 °C; ^1H NMR (300 MHz, DMSO-d_6): δ 9.18 (d, 1H, J = 7.0 Hz), 9.04 (d, 1H, J = 7.0 Hz), 8.87 (s, 1H), 8.37 (d, 1H, J = 8.8 Hz), 7.20 (s, 1H), 7.08 (d, 1H, J = 9.0 Hz), 5.19 (bs, 2H), 3.94 (s, 3H), 3.35 (bs, 2H), 2.97 (q, 2H, J = 7.2 Hz), 2.90 (q, 2H, J = 7.2 Hz), 2.59 (bs, 2H), 1.40 (t, 6H, J = 7.0 Hz). Anal. ($C_{22}H_{25}N_3OI_2$) theoretical: C, 43.95; H, 4.19; N, 6.99. Found: C, 44.27; H, 4.42; N, 7.17.

5.1.3. 12-Carboxymethyl-2,3-diethyl-10-methoxy-pyridazino[1′,6′:1,2]pyrido[3,4-b]indol-5-inium bromide (*1i*)

A mixture of **1f** (see SD) (38.7 mg, 0.08 mmol) and 48% HBr (1 mL) was heated under reflux for 3 h. The solvent was evaporated under reduced pressure and the residue was treated with Et_2O to give **1i** as an orange solid. Yield: 85%; mp: 234–235 °C (ethanol/Et_2O); ^1H NMR (300 MHz, DMSO-d_6): δ 9.33 (d, 1H, J = 6.8 Hz), 8.90 (d, 1H, J = 6.8 Hz), 8.58 (s, 1H), 8.47 (d, 1H, J = 8.9 Hz), 7.68 (s, 1H), 7.17 (d, 1H, J = 8.7 Hz), 5.96 (s, 2H), 3.97 (s, 3H), 3.15 (q, 2H, J = 7.2 Hz), 2.99 (q, 2H, J = 7.2 Hz), 1.39 (t, 6H, J = 6.8 Hz). Anal. ($C_{21}H_{22}N_3O_3Br\cdot H_2O$) theoretical: C, 54.55; H, 5.23; N, 9.09. Found: C, 55.72; H, 5.60; N, 8.77.

5.1.4. 14-Methoxy-16-(pent-4-ynyl)acenaphtho[1″,2″:3′,4′]pyridazino[1′,6′:1,2]pyrido-[3,4-b]indol-9-inium mesitylensulfonate (*1j*)

A mixture of **10** (see SD) (0.10 g, 0.2 mmol), acenaphthoquinone (0.036 g, 0.2 mmol), anhydrous sodium acetate (0.016 g, 0.2 mmol) and ethanol (10 mL) was heated under reflux for 1 h. The solid was filtered when the mixture was still hot and was washed with hot ethanol (5 mL) and hot acetone (5 mL). Crystallization from acetic acid/acetone gave **1j** as an orange solid. Yield: 67%; mp: 273–274 °C; ^1H NMR (300 MHz, DMSO-d_6): δ 9.55 (s, 1H), 9.37 (d, 1H, J = 6.9 Hz), 8.75 (d, 1H, J = 6.9 Hz), 8.71 (d, 1H, J = 6.9 Hz), 8.58 (d, 1H, J = 7.3 Hz), 8.38 (d, 1H, J = 8.4 Hz), 8.34 (d, 2H, J = 8.0 Hz), 8.02 (t, 2H, J = 7.4 Hz), 7.52 (d, 1H, J = 1.8 Hz), 7.18 (dd, 1H, J = 8.8 Hz, J = 2.2 Hz), 5.24 (t, 2H, J = 7.3 Hz), 4.05 (s, 3H), 2.75 (s, 1H), 2.54–2.51 (m, 2H), 2.38–2.29 (m, 2H); IR (KBr): ν 2932, 1621, 1574, 1544, 1409, 1250, 1223, 1161, 829, 678; Anal. ($C_{39}H_{33}N_3O_4S\cdot 2H_2O$) theoretical: C, 69.31; H, 5.52; N, 6.22. Found: C, 69.07; H, 5.19; N, 5.91.

5.1.5. 1,10-Bis-(1-methyl-7-methoxy-pyrido[3,4-b]indol-9-yl)-deca-4,6-diyne (*11*)

A mixture of **9** (see SD) (0.26 g, 1 mmol) and copper(II) acetate (0.90 g, 5 mmol) in acetonitrile (20 mL) was heated under reflux for 48 h. Water (10 mL) and 25% ammonia (5 mL) were added. The mixture was extracted with CH_2Cl_2 (30 mL) and the organic phase was dried ($MgSO_4$) and filtered. The solvent was removed under reduced pressure and the residue was chromatographed on silica gel using acetone/ethanol (8:2) as eluent. Crystallization from acetone gave **11** as a pale yellow solid. Yield: 45%; mp: 184–185 °C; ^1H NMR (300 MHz; $CDCl_3$): δ 8.9 (d, 2H, J = 5.5 Hz), 7.97 (d, 2H, J = 8.8 Hz), 7.74 (d, 2H, J = 5.1 Hz), 6.89 (d, 2H, J = 2.2 Hz), 6.89 (dd, 2H, J = 8.8 Hz, J = 2.2 Hz), 4.64 (t, 4H, J = 7.3 Hz), 3.94 (s, 6H), 3.04 (s, 6H), 2.38 (t, 4H, J = 6.6 Hz), 2.13–2.04 (m, 4H); IR (KBr): ν 2966, 2115, 1617, 1558, 1414, 1238, 1108, 839, 675 cm^{-1}; Anal. ($C_{36}H_{34}N_4O_2$) theoretical: C, 77.95; H, 6.18; N, 10.10. Found: C, 77.71; H, 6.33; N, 9.84.

5.1.6. 9,9′-(Deca-4,6-diyn-1,10-diyl)-bis-(2-amino-1-methyl-7-methoxy-pyrido[3,4-b]indol-2-inium) dimesitylenesulfonate (*12*)

A solution of MSH (0.30 g, 1.4 mmol) in CH_2Cl_2 (2 mL) was added dropwise to a slurry of **11** (0.55 g, 1 mmol) in CH_2Cl_2 (5 mL) at room temperature. After 1 h, Et_2O was added and the resulting solid was filtered and washed with acetone and CH_2Cl_2. Crystallization from ethanol gave **12** as a white solid. Yield: 90%; mp: 250–251 °C; ^1H NMR (300 MHz, DMSO-d_6): δ 8.54 (d, 2H, J = 6.6 Hz), 8.43 (d, 2H, J = 6.9 Hz), 8.30 (d, 2H, J = 9.2 Hz), 7.67 (s, 4H), 7.35 (d, 2H, J = 1.8 Hz), 7.05 (dd, 2H, J = 8.8 Hz, J = 1.8 Hz), 4.70 (t, 4H, J = 7.3 Hz), 3.94 (s, 6H), 3.13 (s, 6H), 2.47–2.43 (m, 4H), 2.02–1.97 (m, 4H); IR (KBr): ν 3432, 3252, 3139, 2934, 2328, 1624, 1573, 1456, 1249, 1228, 1167, 1085, 1014, 816, 679; Anal. ($C_{54}H_{60}N_6O_8S_2$) theoretical: C, 65.83; H, 6.14; N, 8.53. Found: C, 65.57; H, 6.22; N, 8.40.

5.1.7. 12,12′-(Deca-4,6-diyn-1,10-diyl)-bis-(2,3-diethyl-10-methoxy-pyridazino[1′,6′:1,2]pyrido[3,4-b]indol-5-inium) dimesitylenesulfonate (*1k*)

A mixture of **12** (0.10 g, 0.1 mmol), hexane-3,4-dione (0.025 g, 0.2 mmol), anhydrous sodium acetate (0.008 g, 0.1 mmol) and

ethanol (10 mL) was heated under reflux for 24 h. The mixture was evaporated to dryness and the residue was treated with a mixture of acetone/Et_2O. The solid was filtered, washed with cold water (1 mL) and dried under vacuum to give **1k** as a yellow a solid. Yield: 52%; mp: 292–293 °C (ethanol); ^{1}H NMR (300 MHz, CD_3OD): δ 9.10 (d, 2H, J = 6.6 Hz), 8.73 (s, 2H), 8.64 (d, 2H, J = 6.9 Hz), 8.28 (d, 2H, J = 8.8 Hz), 7.20 (d, 2H, J = 2.5 Hz), 7.13 (dd, 2H, J = 8.8 Hz, J = 2.2 Hz), 5.73 (t, 4H, J = 7.5 Hz), 3.99 (s, 6H), 3.16 (q, 4H, J = 7.3 Hz), 3.05 (q, 4H, J = 7.3 Hz), 2.48–2.45 (m, 4H), 2.25–2.18 (m, 4H), 1.51–1.45 (m, 12H); IR (KBr): ν 2954; 1619; 1558; 1414; 1202; 1178; 1085; 679; Anal. ($C_{66}H_{72}N_6O_8S_2 \cdot 1H_2O$) theoretical: C; 68.37; H, 6.43; N, 7.25. Found: C, 68.04; H, 6.69; N, 7.43.

5.1.7.1. General procedure for ester hydrolysis. A mixture of ester **14** or **15** [19] (1 mmol) and 48% HBr (5 mL) was heated under reflux for 2 h. The cooled mixture was filtered and the solid was washed with acetone (2 × 10 mL) and crystallized.

*5.1.8. 9-Carboxymethylacenaphtho[1′,2′:3,4]pyridazine[1,6-a] benzimidazol-14-inium bromide (**2a**)*

Yellow solid. Yield: 93%; mp: 298–300 °C (ethanol/acetone); ^{1}H NMR (300 MHz, DMSO-d_6): δ 9.73 (s, 1H), 8.56–8.48 (m, 3H), 8.38–8.28 (m, 3H), 8.04–7.94 (m, 3H), 7.86 (appt, 1H, J = 7.6 Hz), 5.85 (s, 2H); IR (KBr): ν 3378, 3016, 2907, 2766, 2548, 1752, 1729, 1611, 1528, 1467, 1413, 1374, 1338, 1286, 1215, 1099, 825, 773, 751; Anal. ($C_{22}H_{14}N_3O_2Br \cdot 1/2H_2O$) theoretical: C, 60.12; H, 3.26; N, 9.72. Found: C, 59.87; H, 3.42; N, 9.52.

*5.1.9. 9-(3-Carboxypropyl)acenaphtho[1′,2′:3,4]pyridazine[1,6-a] benzimidazol-14-inium bromide (**2b**)*

Yellow solid. Yield: 94%; mp: 299–300 °C (ethanol/acetone); ^{1}H NMR (300 MHz; DMSO-d_6): δ 9.74 (s, 1H), 8.62 (d, 1H, J = 7.0 Hz), 8.56 (d, 1H, J = 8.2 Hz), 8.41 (d, 1H, J = 8.2 Hz), 8.40 (d, 1H, J = 8.2 Hz), 8.32 (d, 1H, J = 8.2 Hz), 8.06–8.00 (m, 2H), 7.97 (appt, 1H, J = 7.8 Hz), 7.86 (appt, 1H, J = 7.5 Hz), 4.90 (t, 2H, J = 7.0 Hz), 2.51 (t, 2H, J = 7.3 Hz), 2.28–2.20 (m, 2H); IR (KBr): ν 3380, 2960, 1722, 1629, 1607, 1528, 1419, 1401, 1299, 1205, 1180, 1100, 830, 762; Anal. ($C_{24}H_{18}N_3O_2Br \cdot 3/2H_2O$) theoretical: C, 59.15; H, 4.34; N, 8.62. Found: C, 59.17; H, 4.35; N, 9.01.

*5.1.10. 9-(3-Bromopropyl)acenaphtho[1′,2′:3,4]pyridazino[1,6-a] benzimidazol-14-ium bromide (**17**)*

A slurry of **16** (see SD) (0.06 g, 0.2 mmol) in 1,3-dibromopropane (2.01 g, 10 mmol) was heated by microwave irradiation for 10 min at 300 W. The precipitate was filtered when the mixture was still hot and was washed with acetone. The solid was crystallized from ethanol to give **17**. Yield: 90%; mp: 231–233 °C; ^{1}H NMR (300 MHz; DMSO-d_6): δ 9.70 (s, 1H), 8.66–8.57 (m, 3H), 8.44 (d, 2H, J = 8.4 Hz), 8.33 (d, 1H, J = 8.4 Hz), 8.10–8.03 (m, 2H), 7.97 (appt, 1H, J = 8.0 Hz, J = 7.3 Hz), 7.87 (appt, 1H, J = 8.4 Hz, J = 7.3 Hz), 4.97 (t, 2H, J = 7.3 Hz), 3.67 (t, 2H, J = 7.3 Hz), 2.55–2.50 (m, 2H); ^{13}C NMR (75 MHz; DMSO-d_6): δ 153.2, 140.3, 139.5, 136.8, 132.5, 132.0, 131.9, 130.6, 130.5, 130.4, 130.4, 129.8, 129.2, 128.9, 127.1, 126.1, 124.2, 114.0, 113.9, 112.0, 40.6, 32.7, 32.7, 31.3; IR (KBr): ν 3416, 2941, 2892, 1628, 1610, 1529, 1480, 1425, 1245, 1165, 1098, 1034, 817, 778, 750, 636; Anal. ($C_{23}H_{17}N_3Br_2 \cdot 1H_2O$) theoretical: C, 53.82; H, 3.73; N, 8.18. Found: C, 53.90; H, 3.81; N, 8.26.

*5.1.11. 9-(4,4,8-Trimethyl-8-aza-4-azonium-nonanyl)acenaphtho [1′,2′:3,4]-pyridazino[1,6-a]benzimidazol-14-inium dibromide (**2c**)*

A mixture of **17** (0.19 g, 0.4 mmol) and *N*,*N*,*N*,*N*-tetramethyl-propane-1,3-diamine (0.025 g, 0.2 mmol) in DMF (20 mL) was heated at 90–100 °C for 72 h. The solvent was removed under reduced pressure and the residual solid was chromatographed on silica gel using methanol/dichloromethane (10:1) as an eluent to give **2c** as a pale yellow solid. Yield: 46%; mp: >300 °C; ^{1}H NMR (300 MHz; DMSO-d_6): δ 10.28 (s, 1H), 8.78 (d, 1H, J = 6.9 Hz), 8.58 (d, 1H, J = 6.2 Hz), 8.47–8.41 (m, 3H), 8.06–7.96 (m, 3H), 7.88 (appt, 2H, J = 8.0 Hz, J = 7.2 Hz), 5.04 (bs, 2H), 3.68–3.78 (m, 2H), 3.47–3.34 (m, 2H), 3.09 (s, 6H), 3.05 (bs, 2H), 2.79 (s, 6H), 2.79–2.68 (m, 2H), 2.28–2.16 (m, 2H); ^{13}C NMR (75 MHz; DMSO-d_6): δ 155.0, 144.8, 139.4, 138.1, 135.4, 131.1, 130.9; 130.7; 129.3; 129.2; 129.1; 129.0; 127.8; 127.6; 125.9; 125.1; 123.0; 114.0; 113.0; 112.7, 49.9, 46.2, 45.2, 41.3, 26.1, 21.7, 19.3, 19.1, 17.3; IR (KBr): ν 3419, 3013, 1611, 1529, 1467, 1099, 1036, 828, 760; Anal. ($C_{30}H_{35}N_5Br_2 \cdot 2H_2O$) theoretical: C, 54.47; H, 5.94; N, 10.59. Found: C, 54.73; H, 5.83; N, 10.70.

5.2. Biological assays

5.2.1. Cell line, human primary cells and reagents

The human promonocytic cell line THP-1 was grown in RPMI-1640 medium (Lonza, Verviers, Belgium) supplemented with 5% (v/v) heat-inactivated FCS (HyClone, Cramlington, UK).

PBMCs were isolated from healthy donors by Ficoll/Hypaque (GE Healthcare Bio-Sciences AB, Uppsala, Sweden) density gradient centrifugation and were cultured in RPMI-1640 plus 10% FCS. $CD14^+$ cells were purified from PBMCs using CD14 human Microbeads (Miltenyi Biotec, Bergisch-Gladbach, Germany). Flow cytometry analysis of isolated PMBCs and monocytes showed that cell purity was at least 95%. To induce differentiation into immature DCs, $CD14^+$ cells were cultured in the presence of recombinant human GM-CSF (500 U/mL) and recombinant human IL-4 (100 U/mL) (PeproTech, London, UK). After 3 days of culture, fresh medium containing GM-CSF and IL-4 was added, and the incubation was prolonged for 2 days. Differentiation was assessed by flow cytometry analysis of specific markers (loss of CD14, and acquisition of CD23 and CD1a).

LPS and propidium iodide were purchased from Sigma–Aldrich (St. Louis, MO). LPS was dissolved in PBS. Newly synthesised compounds were dissolved in DMSO as 100 mM stock solutions and these were stored at −20 °C.

5.2.2. Cell treatment, viability and cytokine determination

THP-1 cells were incubated for 24 h in RPMI-1640 plus 5% FBS and 10 μM of the various compounds. Duplicate cultures were stimulated with 100 ng/mL LPS during the last 4 h. Cell viability was measured in each case by flow cytometry through the determination of the percentage exclusion of propidium iodide (0.5 μg/mL). Cells were analysed in a FACScalibur cytofluorometer using CellQuestPro software (BD Bioscience, San Jose, CA, USA).

The production of TNF-α was quantified in culture supernatants of cells incubated for 24 h in the presence of increasing concentrations of the selected compounds and stimulated with 100 ng/mL LPS (THP-1 cell line) or 10 ng/mL LPS (primary cells) during the last 4 h. Poly I:C (10 μg/mL) stimulation was carried out overnight. Cell-free supernatants were collected and the cytokine content was evaluated by using the Human TNF ELISA Set (BD Bioscience) according to the manufacturer's instructions. A standard curve was prepared with known concentrations of human TNF-α. Optical density (OD_{450nm}) was measured in a Synergy4 plate reader and results were analysed using Gen5 software (BioTek).

The percentage inhibition was calculated as 100 − ([TNF (pg/mL) in the presence of compound/maximum of TNF (pg/mL)] × 100). Linear regression was used to calculate the IC_{50} value for each cell population.

The concentration of IL-12 in the supernatant of poly I:C stimulated DCs was measured by flow cytometry using the human IL-12 Cytometric Bead Array (CBA) Flex Set kit (BD, Biosciences, CA) according to the manufacturer's instructions.

5.2.3. Quantitative RT-PCR analysis of TNF-α gene expression

Isolated $CD14^+$ human monocytes were incubated overnight in the presence of compound **1e** (1 μM) or vehicle and stimulated with LPS (10 ng/mL) during an extended period of 2 h. After this time, cells were harvested, total RNA was isolated using a High Pure RNA Isolation kit (Roche, Indianapolis, IN, USA), and reverse-transcribed with random hexamers and avian myeloblastosis virus-reverse transcriptase (Roche, Indianapolis, IN, USA) in a final volume of 20 μL for 1 h at 42 °C. TNF-α and β2-microglobulin mRNA expression were quantified by real real-time PCR in a Light Cycler (Roche, Indianapolis, IN) with FastStart DNA Master SYBR Green (Roche, Indianapolis, IN). Primers used were as follows: 5′-GAA AGG ACA CCA TGA GCA CTG-3′ and 5′-TGA TTA GAG AGA GGT CCC TGG-3′ for TNF-α and 5′-CCA GCA GAG AAT GGA AAG TC-3′ and 5′-GAT GCT GCT TAC ATG TCT CG-3′ for β2-microglobulin. Standard curves for TNF-α and β2-microglobulin mRNA quantification were generated by amplifying 10-fold serial dilutions of known quantities of the specific PCR products. Relative units estimated from the quantification represent the ratio of TNF-α mRNA molecules to β2-microglobulin mRNA molecules in the same cDNA sample.

5.2.4. In vivo assay

Female C57BL/6 mice (Charles River, Barcelona, Spain) were used for *in vivo* studies. Animals were housed in ventilated cages to minimise contact with pathogens. Mice weighing about 20 gr and 8–9 weeks old were treated by intraperitoneal injection with 2 doses of compound **1e** (2 mg/kg) dissolved in 200 μL of saline solution at 18 h intervals. Control animals received a similar volume of vehicle in saline solution. Four hours after the second dose, the mice were sacrificed and the spleens were removed. Splenocytes were prepared by mechanical dissociation. Single cell suspensions were obtained after filtration through a 70 μM cell strainer (BD). Splenocytes from **1e**-treated and control vehicle-treated mice were counted and cultured at 10^6 cells/mL in RPMI-1640/5% FBS. Duplicate cultures were stimulated with 10 ng/mL LPS during 4 h and secreted TNF-α was measured in cell free culture supernatants using the murine TNF-α Cytometric Bead Array (CBA) Flex Set kit (BD, Biosciences, CA).

Acknowledgements

The work described in this paper was partially supported by grants SAF 2010/19867 (Spanish Ministerio de Economía y Competitividad) to T.B.; FIS 09/00641, REDinREN 2.0 FEDER and Reina Sofía Institute of Nephrology Research (IRSIN) monetary funds to R.S.; CTQ2011-24715 (Spanish Ministerio de Economía y Competitividad) and REDinREN RD12/0021/0014 (Instituto de Salud Carlos III) to J.J.V., and a fellowship to P.S-A. (University of Alcalá). The authors would like to thank Juliette Siegfried and her team at ServingMed.com for their editing of the manuscript.

Appendix A. Supplementary data

Supplementary data related to this article can be found at http://dx.doi.org/10.1016/j.ejmech.2015.01.060.

References

[1] D. Robinson Jr., M. Hackett, J. Wong, A.B. Kimball, R. Cohen, M. Bala, Co-occurrence and comorbidities in patients with immune-mediated inflammatory disorders: an exploration using US healthcare claims data, 2001-2002, Curr. Med. Res. Opin. 22 (2006) 989–1000.
[2] T. Kawai, S. Akira, Signaling to NF-kappaB by Toll-like receptors, Trends Mol. Med. 13 (2007) 460–469.
[3] F. Balkwill, B. Foxwell, F. Brennan, TNF is here to stay!, Immunol. Today 21 (2000) 470–471.
[4] A. Kuek, B.L. Hazleman, A.J. Ostor, Immune-mediated inflammatory diseases (IMIDs) and biologic therapy: a medical revolution, Postgrad. Med. J. 8 (2007) 251–260.
[5] H. Tilg, A.R. Moschen, Adipocytokines: mediators linking adipose tissue, inflammation and immunity, Nat. Rev. Immunol. 6 (2006) 772–783.
[6] P. Dandona, A. Aljada, A. Bandyopadhyay, Inflammation: the link between insulin resistance, obesity and diabetes, Trends Immunol. 25 (2004) 4–7.
[7] M. Saghizadeh, J.M. Ong, W.T. Garvey, R.R. Henry, P.A. Kern, The expression of TNF alpha by human muscle. Relationship to insulin resistance, J. Clin. Invest. 97 (1996) 1111–1116.
[8] K.T. Uysal, S.M. Wiesbrock, M.W. Marino, G.S. Hotamisligil, Protection from obesity-induced insulin resistance in mice lacking TNF-alpha function, Nature 389 (1997) 610–614.
[9] L.C. Silva, L.C. Ortigosa, G. Benard, Anti-TNF-alpha agents in the treatment of immune-mediated inflammatory diseases: mechanisms of action and pitfalls, Immunotherapy 2 (2010) 817–833.
[10] L. Hsu, B.T. Snodgrass, A.W. Armstrong, Antidrug antibodies in psoriasis: a systematic review, Br. J. Dermatol. 170 (2014) 261–273.
[11] M.A. Palladino, F.R. Bahjat, E.A. Theodorakis, L.L. Moldawer, Anti-TNF-α Therapies: the next generation, Nat. Rev. Drug Discov. 2 (2003) 736–746.
[12] P.L. Toogood, Inhibition of protein-protein association by small molecules: approaches and progress, J. Med. Chem. 45 (2002) 1543–1558.
[13] T. Berg, Modulation of protein-protein interactions with small organic molecules, Angew. Chem. Int. Ed. Engl. 42 (2003) 2462–2481.
[14] K.S. Kumar, P.M. Kumar, K.A. Kumar, M. Sreenivasulu, A.A. Jafar, D. Rambabu, G.R. Krishna, C.M. Reddy, R. Kapavarapu, K. Shivakumar, K.K. Priya, K.V.L. Parsa, M. Pal, A three-component reaction: green synthesis of novel isoindolo[2,1-a]quinazoline derivatives as potent inhibitors of TNF-α, Chem. Commun. 47 (2011) 5010–5012.
[15] K.S. Kumar, P.M. Kumar, M.A. Reddy, Md Ferozuddin, M. Sreenivasulu, A.A. Jafar, G.R. Krishna, C.M. Reddy, D. Rambabu, K.S. Kumar, S. Pal, M. Pal, $Y(OTf)_3$ catalyzed new cascade reaction: a facile assembly of fused quinazolinones, Chem. Commun. 47 (2011) 10263–10265.
[16] D.S.-H. Chan, H.-M. Lee, F. Yang, C.-M. Che, C.C.L. Wong, R. Abagyan, C.-H. Leung, D.-L. Ma, Structure-based discovery of natural-product-like TNF-α inhibitors, Angew. Chem. Int. Ed. 49 (2010) 2860–2864.
[17] M.M. He, A.S. Smith, J.D. Oslob, W.M. Flanagan, A.C. Braisted, A. Whitty, M.T. Cancilla, J. Wang, A.A. Lugovskoy, J.C. Yoburn, A.D. Fung, G. Farrington, J.K. Eldredge, E.S. Day, L.A. Cruz, T.G. Cachero, S.K. Miller, J.E. Friedman, I.C. Choong, B.C. Cunningham, Small-molecule inhibition of TNF-a, Science 310 (2005) 1022–1025.
[18] A. Fontana, E.J. Benito, M.J. Martín, N. Sánchez, R. Alajarín, J.J. Vaquero, J. Álvarez-Builla, S. Lambel-Giraudet, S. Leonce, A. Pierré, D. Caignard, Synthesis and cytotoxic activity of pyridazino[1′,6′:1,2]pyrido[3,4-*b*]indol-5-inium derivatives as anti-cancer agents, Bioorg. Med. Chem. Lett. 12 (2002) 2611–2614.
[19] J. Pastor, J. Siro, J.L. García-Navío, J.J. Vaquero, J. Álvarez-Builla, F. Gago, B. de Pascual-Teresa, M. Pastor, M.M. Rodrigo, Azino-fused benzimidazolium salts as DNA intercalating agents, J. Org. Chem. 62 (1997) 5476–5483.
[20] J. Álvarez-Builla, J.J. Vaquero, J.L. García-Navío, J.F. Cabello, C. Sunkel, M. Faude Casa Juana, F. Dorrego, L. Santos, 1,5-bis-[*N*-benzyl-*N*,*N*-diethylamonio)-3-oxapentane dichloride, a novel bis-amonnium salt as phase transfer catalyst, Tetrahedron 46 (1990) 967–978.
[21] J. Pastor, J. Siro, J.L. García-Navío, J.J. Vaquero, M.M. Rodrigo, M. Ballesteros, J. Álvarez-Builla, Synthesis of new azino fused benzimidazolium salts. A new family of DNA intercalating agents I, Bioorg. Med. Chem. Lett. 5 (1995) 3043–3048.
[22] J. Siro, J. Pastor, J.L. García-Navío, J.J. Vaquero, J. Álvarez-Builla, Unexpected N-C bond fission of fused N-alkylbenzimidazolium salts. A new approach to pyrido[1,2-*a*]- or pyridazino[1,6-*a*]benzimidazoles, Tetrahedron 54 (1998) 1929–1936.
[23] R.L. Funk, E.R.R. Young, R.M. Williams, M.F. Flanagan, T.L. Cecil, Photochemical cycloaromatization reactions of ortho-dialkynylarenes. A new class of DNA photocleaving agents, J. Am. Chem. Soc. 118 (1996) 3291–3292.
[24] R. Ekkebus, S.I. van Kasteren, Y. Kulathu, A. Scholten, I. Berlin, P.P. Geurink, A. de Jong, S. Goerdayal, J. Neefjes, A.J.R. Heck, D. Komander, H. Ovaa, On terminal alkynes that can react with active-site cysteine nucleophiles in proteases, J. Am. Chem. Soc. 135 (2013) 2867–2870.